ELSEVIER

Chemical Engineering Science 61 (2006) 1092–1101

Chemical Engineering Science

www.elsevier.com/locate/ces

A miniaturized methanol reformer with Si-based microreactor for a small PEMFC

Yoshihiro Kawamura[a, b, *], Naotsugu Ogura[a], Tadao Yamamoto[a], Akira Igarashi[b]

[a] *CASIO Computer Co., Ltd., 3-2 Fujihashi 3-chome, Ome-shi, Tokyo 198-0022, Japan*

[b] *Department of Environmental Chemical Engineering, Kogakuin University, 2665-1 Nakano-machi, Hachioji-shi, Tokyo 192-0015, Japan*

Received 14 April 2005; received in revised form 1 August 2005; accepted 10 August 2005
Available online 23 September 2005

Abstract

A miniaturized methanol reformer with $Cu/ZnO/Al_2O_3$ catalyst-based microreactor suitable for the supply of hydrogen for a small proton exchange membrane fuel cell is designed and fabricated using microfabrication techniques. The microreactor ($25 \times 17 \times 1.3\,mm^3$) is constructed from glass and silicon substrates to form a serpentine catalyst-coated microchannel of 333 mm in length and cross-section of $0.6 \times 0.4\,mm^2$, designed based on mass and heat balance analyses using a one-dimensional model. The use of the high-performance $Cu/ZnO/Al_2O_3$ catalyst allows for higher hydrogen production rates than possible using a commercial Cu/ZnO catalyst. The microreactor is demonstrated to be capable maintaining a hydrogen production rate suitable for powering 1 W-class devices such as cellular phones.

Keywords: Microreactors; Microfabrication; Fuel processing; Reaction engineering; Methanol reforming; Catalysis

1. Introduction

Various portable electronic devices have recently come into popular use, and the performance of these devices has improved remarkably. However, greater performance leads to greater consumption of electrical power, and it has become difficult to secure a sufficiently long-lasting power source for these portable electronic devices. This is often true even when a conventional lithium-ion battery is used, despite the higher energy density compared to other secondary batteries. This energy demand is also expected become more severe with the advent of broadband network devices in a ubiquitous computing environment, and the higher power consumption contributes to environmental pollution arising from the mass disposal of expended batteries. Long-life batteries offering high efficiency and reduce environmental impact are therefore in demand.

The proton exchange membrane fuel cell (PEMFC) has attracted much attention as a potential power source for portable electronic devices. The fuels targeted as energy resources for PEMFCs have potentially high volumetric energy densities, up to $2500\,W\,h\,l^{-1}$ for liquid hydrogen or $5000\,W\,h\,l^{-1}$ for methanol, compared to $400\,W\,h\,l^{-1}$ provided by lithium-ion batteries (Dyer, 2004). At a system level, fuel cell systems are capable of up to 12 times the gravimetric energy density of conventional lithium-ion batteries (Dyer, 2002). As an annual market of over $10 billion with a growth rate of 40% per annum is estimated for power sources suitable for new portable electronic devices (Dyer, 2002), researchers have been encouraged to investigate miniaturized fuel cell systems. Two types of small PEMFC systems have been proposed: direct methanol systems and reforming systems. Direct methanol systems have the advantage of room-temperature operation but offer only relatively low power density due to methanol crossover through the polymer electrolyte membrane and the low reaction rate of methanol oxidation over the anode electrocatalyst. In contrast, reforming systems generate electrical energy in the fuel cell from concentrated hydrogen produced

* Corresponding author. CASIO Computer Co., Ltd., 3-2 Fujihashi 3-chome, Ome-shi, Tokyo 198-0022, Japan. Tel.: +81 428 32 1741; fax: +81 428 31 7651.

E-mail address: kawamuy@rd.casio.co.jp (Y. Kawamura).

0009-2509/$ - see front matter © 2005 Elsevier Ltd. All rights reserved.
doi:10.1016/j.ces.2005.08.014

by steam reforming, for example, from methanol. Reforming systems achieve high power density but are difficult to miniaturize due to the complexity of the required structure, which includes not only a fuel reformer but also a vaporizer, a CO removal unit, and various peripheral parts. Although a few researchers have attempted to miniaturize a hydrogen producer for small power sources (Holladay et al., 2002; Hu et al., 2003), temperatures exceeding 300 °C, which is clearly too high for portable device applications, are required for the process, even when methanol, which enables operation at relatively low temperatures, is used as the hydrogen source. Thus, neither of these systems are suitable as yet for practical application as power sources for portable electronic devices.

Recently, microreactor systems with microchannel reaction fields have generated interest (Ehrfeld et al., 2000). This type of microreactor is superior to conventional reactors in that it has a higher specific surface area and shorter diffusion length, and also allows for reactions that were previously difficult to achieve (Igarashi, 2002). The microfabrication of channels on a single substrate also allows the various components of the microreactor, such as heat sources, electronic controllers, driving units, sensors, and microvalves to be integrated with semiconductor technology and microelectromechanical system (MEMS) technology (Kusakabe and Morooka, 2002). It may now be feasible to miniaturize the complicated reformer as a microreactor for a small PEMFC, and several investigations have recently been launched (Tanaka et al., 2004; Pavio, 2003; Park et al., 2004; Reuse et al., 2004). It may also be possible, through the use of these technologies, to achieve sufficient thermal insulation between the reformer (with microreactor) and the periphery of the system (where the surface temperature should be comfortable to the touch). It is therefore expected that small PEMFC systems with high power density, sufficient to power portable electronic devices, will be realized in the near future.

However, the large specific surface area of the microreactor results in heat release (i.e., heat loss) at rates comparable to the effective heat transfer in the microreactor system. Therefore, when an endothermic reaction occurs in the microreactor, which requires heat supply from a heat source, the effective utilization of heat becomes more important than in a conventional reactor. In terms of heat efficiency, methanol is the most appropriate fuel for a miniaturized reformer with microreactor as it allows for low-temperature operation in hydrogen production. Furthermore, a high-performance $Cu/ZnO/Al_2O_3$ catalyst developed previously by our group (Kawamura et al., 2005) should allow hydrogen production at a lower temperature than achievable using commercial catalysts. It is thus expected that the improved energy efficiency of this high-performance catalyst will lead to the development of microreactor hydrogen production suitable for use as a power source for portable electronic devices. In this study, a miniaturized methanol reformer with microreactor is constructed using the $Cu/ZnO/Al_2O_3$ catalyst for low-temperature hydrogen production.

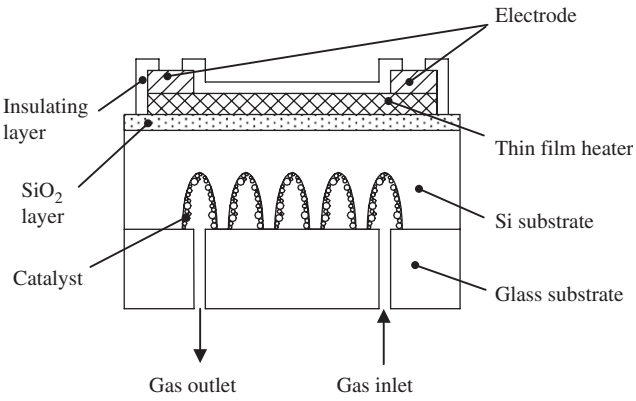

Fig. 1. Structure of microreactor.

2. Experimental

2.1. Construction of microreactor

Fig. 1 shows the structure of the microreactor. Silicon and glass (#7740, Corning) substrates were selected as components of the microreactor. These materials have adequate thermal tolerance to handle the temperature of methanol reforming, and also allow the fabrication process to be simplified by being suitable for sandblasting for microchannel fabrication and anodic bonding at moderate temperatures for junction forming, thereby preventing possible thermal degradation of the catalyst deposited in the microchannel. These issues have proven to be problematic for ceramic (Pavio, 2003) and metallic (Park et al., 2004; Reuse et al., 2004) microreactors. A metal oxide (Ta–Si–O–N) was formed on the Si substrate as a thin film heater, which has the advantage of reaction temperature regulation due to its high resistivity (4 mΩ cm) (Tanaka et al., 2001, 2005).

The microreactor was 25 mm long, 17 mm wide, and 1.3 mm thick, with weight of approximately 1.0 g. The microchannel formed on the Si substrate was 333 mm long, 0.6 mm wide, and 0.4 mm deep. The glass substrate, with a gas inlet and outlet of 0.5 mm in diameter, was connected to the Si substrate to complete the microchannel. The length of the microchannel was determined by mass and heat balance equations based on a one-dimensional model assuming the prescribed width and depth of the microchannel, as described later.

2.2. Microreactor process

Fig. 2 shows the processing flow for fabrication of the microreactor. The thin film heater and electrode was formed first by sputtering Ta–Si–O–N (heater) and Au (electrode) films onto a thin SiO_2 layer on one side of a Si wafer

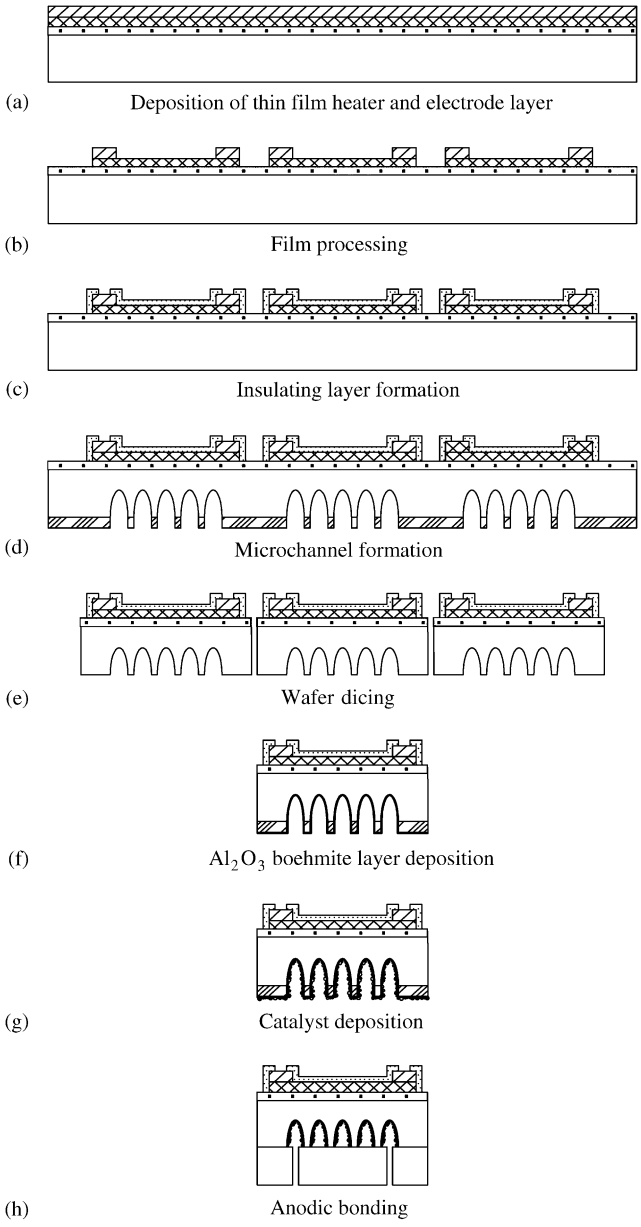

Fig. 2. Processing flow for microreactor fabrication.

(polished on both sides) (Fig. 2(a)). Each film was then shaped respectively by photolithography (Fig. 2(b)). To prevent the thin film heater from coming into physical contact with the electrode, which could result in destruction of the films or a short circuit, an insulating layer (Ta–Si–O) was formed on the heater side of the Si substrate, leaving several areas uncoated as electrical contacts (Fig. 2(c)).

A dry-film photoresist was then fixed to the microchannel side of the Si wafer and shaped by photolithography. The serpentine microchannel was then formed by sandblasting using #400 SiC particles (Fig. 2(d)). Subsequently, the substrate was ultrasonicated in a hot alkaline aqueous solution to remove the dry-film photoresist. The final processed Si wafer was divided into several pieces by dicing (Fig. 2(e)).

The high-performance $Cu/ZnO/Al_2O_3$ catalyst for methanol reforming was then deposited in the microchannel. The preparation of the catalyst is described in the previous report (Kawamura et al., 2005). Briefly, the catalyst was prepared from a precursor coprecipitated by the simultaneous dropping of a mixed solution of copper and zinc nitrate and an aqueous solution of Na_2CO_3 into an Al_2O_3 boehmite suspension (Cu/Zn/Al $= 6/3/1$ mol ratio). The catalyst prepared under optimal conditions for high Cu interdispersion with ZnO and large Cu surface area performs at a lower operating temperature than the commercial catalyst. The selective deposition of the catalyst in the microchannel was performed by applying a dry-film photoresist on the microchannel side such that only the microchannel was exposed. A thin Al_2O_3 boehmite layer was then formed on the microchannel by dip coating using an Al_2O_3-sol prepared by hydrolysis of aluminum isopropoxide to increase the adhesive strength between the catalyst and the microchannel wall (Fig. 2(f)). After drying of Al_2O_3 boehmite layer at 100 °C, the high-performance $Cu/ZnO/Al_2O_3$ catalyst for methanol reforming was deposited in the microchannel by dip coating using a slurry of the catalyst (Fig. 2(g)). The slurry was prepared by adding a powder of the catalyst produced by pounding in an agate mortar to distilled water along with a small amount of hydroxyethyl cellulose to improve dispersion. After drying the catalyst layer, the dry-film photoresist was mechanically peeled from the Si substrate, and the workpiece was calcined at 350 °C. A commercial Cu/ZnO catalyst (MDC-3, Süd-Chemie) was also deposited in the microchannel by a similar procedure as a reference. The state of the catalyst in the microchannel was analyzed by scanning electron microscopy (SEM; S-4200, Hitachi) and energy dispersive X-ray (EDX) fluorescence spectrometry (EMAX-7000, Horiba).

Finally, the Si substrate and glass substrate, in which the gas inlet and outlet ports were fabricated by sandblasting, were connected by anodic bonding (Fig. 2(h)). Anodic bonding was conducted at an impress voltage of 1500 V and a bonding temperature of 350 °C.

2.3. Methanol reforming with microreactor

The test system for methanol reforming using the microreactor is shown in Fig. 3. The microreactor was fastened to a stainless steel (SUS304) holder with flow channels. The gap between the gas ports of the microreactor and holder was sealed with a rubber gasket. The microreactor was heated by applying direct current to the thin film heater, and the temperature of the microreactor was measured by a thermocouple fixed to the glass substrate on the microchannel side. Prior to methanol reforming, the catalyst was reduced under H_2 flow at 250 °C for 20 min, followed by purging with N_2. A methanol aqueous solution (steam/methanol ratio, i.e., steam/carbon (S/C) ratio $= 2.0\,\mathrm{mol\,mol^{-1}}$) was then fed to the microreactor by a micro feeder through a

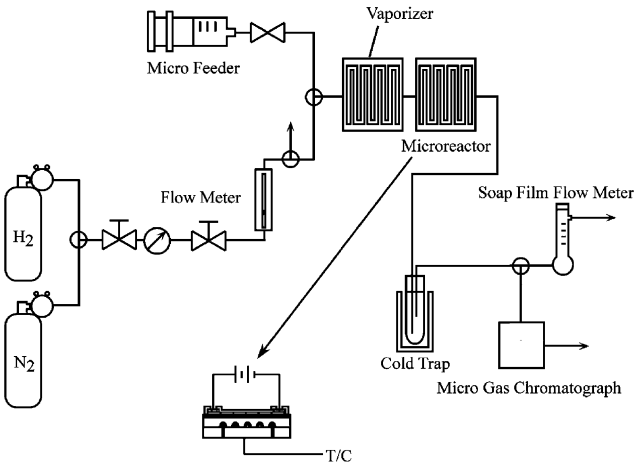

Fig. 3. Schematic of microreactor system for methanol reforming.

vaporizer composed of a dummy microreactor without a catalyst layer. The performance of the microreactor was evaluated for a liquid-based feed rate of 0.25 to 3.2 ml h^{-1}. After separation of the liquid components (methanol and water) by a cold trap set in an ice–water bath, the flow rate of the produced gas was measured by a soap film flow meter, and the reformate was analyzed using a thermal conductivity detector (TCD)-type gas chromatograph (CP-2002, Varian; with MolSieve 5A and Pora PLOT Q columns).

3. Results and discussion

3.1. Determination of microchannel design

The length of the microchannel was determined through simulations of methanol reforming using mass and heat balance equations based on a one-dimensional model for an incompressible fluid. The rate equation of methanol steam reforming (1) for the simulation is expressed as Eq. (2)

$$CH_3OH + H_2O \rightarrow 3H_2 + CO_2,$$
$$\Delta H^0_{298} = 49.5 \times 10^3\ \mathrm{J\,mol^{-1}}, \quad (1)$$

$$r_{SR} = \frac{\eta \rho_{cat} \delta(w + 2h + 2\delta)}{wh} k_0 \exp\left(-\frac{E_a}{RT}\right) \times (RT)^{0.09} C_A^{0.26} C_B^{0.03} C_C^{-0.2}, \quad (2)$$

where r_{SR} is the rate of the methanol steam reforming reaction, η is the effectiveness factor of the catalyst, ρ_{cat} is the bulk density of the catalyst (1.6×10^3 kg m^{-3} in this study), δ is the thickness of the catalyst layer, and w and h are the cross-sectional width and depth of the microchannel with the catalyst layer, respectively. Hence, in Eq. (2),

$$\frac{\rho_{cat}\delta(w + 2h + 2\delta)}{wh},$$

represents the catalyst weight per unit volume of the microchannel with the catalyst layer. k_0 and E_a are the frequency factor and activation energy, which are determined by a fitting of the experimental results as described later. C_A, C_B, and C_C are the concentrations of reactant A, B, and C (in this case, methanol, water, and hydrogen). The orders of reactions in methanol, water, and hydrogen (0.26, 0.03, and −0.2, respectively) were obtained from the report of Jiang et al. (1993), according to whom the reaction rate of methanol reforming over the $Cu/ZnO/Al_2O_3$ catalyst can be expressed as an Arrhenius-type equation as follows:

$$r = k_0 \exp\left(-\frac{105 \times 10^3}{RT}\right) P_{MeOH}^{0.26} P_{H_2O}^{0.03} P_{H_2}^{-0.2}. \quad (3)$$

Several literatures (Samms and Savinell, 2002; Purnama et al., 2004; Lee et al., 2004) also agree that the rate equation of methanol reforming over a $Cu/ZnO/Al_2O_3$ is described as an Arrhenius-type equation with a power low expression. Jiang et al. (1993) concluded that while an inhibiting effect of hydrogen was observed as shown in Eq. (3), carbon dioxide was found to have no effect. Jiang et al. (1993) also found, by referring to the reaction mechanism proposed by Takahashi et al. (1982), that carbon monoxide has very little effect on the reaction rate, thereby suggesting the rate equation can be expressed as Eq. (3). In our previous report (Kawamura et al., 2005), the concentration of carbon monoxide in the reformed gases over the high-performance $Cu/ZnO/Al_2O_3$ catalyst used in this study also did not exceed the equilibrium concentration, which agrees that methanol reforming over the $Cu/ZnO/Al_2O_3$ catalyst proceeds along with the mechanism proposed by Takahashi et al. (1982). Further, our previous report (Kawamura et al., 2005) observed no methane production over the $Cu/ZnO/Al_2O_3$ catalyst, therefore the methanation was not considered in the present investigation.

The mass and heat balance equations are expressed as

$$uC_{A0}\frac{dx_A}{dz} = -r_A, \quad (4)$$

$$u\rho h c_{pm}\frac{dT}{dz} = q - h(-r_A)\Delta H_r, \quad (5)$$

where u is the flow rate of gases, C_{A0} is the concentration of reactant A at the inlet, x_A is the conversion of reactant A, z is the longitudinal position from the inlet, $-r_A$ is set to equal r_{SR}, ρ is the fluid density, c_{pm} is the fluid specific heat, q is the heat flux, and ΔH_r is the heat of reaction. The boundary conditions for Eqs. (4) and (5) were defined as $u = u_0$ and $T = T_0$ at $z = 0$.

The kinetic parameters of E_a, and k_0 in Eq. (2) were calculated by a fitting of preliminary experimental results (Table 1) for methanol conversion at various temperatures. As a result, E_a and k_0 were determined to be 114.5×10^3 J mol^{-1} and 1.63×10^{10} mol kg^{-1} s^{-1} $Pa^{-0.09}$, respectively.

Next, the dimensions of the microchannel were analyzed based on the simultaneous Eqs. (4) and (5) with respect to rate Eq. (2). The effectiveness factor of catalyst was

Table 1
Pre-experimental result of methanol reforming at various temperatures using microreactor

Reaction temperature/°C	Methanol conversion[a]/%
200	16.4
225	52.3
250	100.0

Feed rate of methanol: 8.9×10^{-7} mol s^{-1}.
S/C : 1.2 mol mol^{-1}.
[a]Catalyst weight: 11 mg.

assumed to be 1, the catalyst layer was assumed to be 15 μm thick, and the cross-sectional width and depth of the microchannel without the catalyst layer were set at 0.6 and 0.4 mm, respectively. The methanol conversion and gas concentration were then calculated for a methanol flow rate of 0.013 mol h^{-1}, corresponding to a liquid-based flow rate of 1.0 ml h^{-1} (S/C = 2.0 mol mol^{-1}) at the inlet. At this flow rate, methanol conversion of almost 100% provides a hydrogen production rate sufficient to power a cellular phone (1 W). Therefore, $u_0 = 2.3$ m s^{-1} was set as the boundary condition for Eqs. (4) and (5), and the inlet temperature was set at 280 °C on the basis of previous catalytic activity tests (Kawamura et al., 2005). For a reforming temperature of 280 °C, calculations using thermodynamic data gave a fluid density and fluid specific heat of the gas composition at the inlet of 0.49 kg m^{-3} and 2.02×10^3 J kg^{-1} K^{-1}, respectively. These values were used in Eq. (5). A heat flux of 1200 J m^{-2} s^{-1} was set to ensure that the microreactor temperature could be maintained at 280 °C, and this value was also applied in Eq. (5).

The calculation results are shown in Fig. 4(a) and (b). Methanol reforming progresses in approximate proportion to the longitudinal position from the inlet at 280 °C, with almost complete methanol conversion obtained 330 mm from the inlet. The microchannel of the miniaturized methanol reformer was therefore determined to be 333 mm long for this width (0.6 mm) and depth (0.4 mm).

The influence of diffusion in the catalyst layer was also considered. The average pore diameter of the high-performance Cu/ZnO/Al_2O_3 catalyst, as determined from the adsorption isotherm for N_2 at −196 °C measured using a volumetric absorption apparatus (ASAP2010, Micromeritics), is 9 nm, which is smaller than one tenth of the mean free path. Thus, Knudsen diffusion dominates in the catalyst layer, and the effective diffusion coefficient can be expressed as

$$D_{eA} = 3.067 r_e \frac{\varepsilon}{\tau}\sqrt{\frac{T}{M_A}}, \tag{6}$$

where D_{eA} is the effective diffusion coefficient of reactant A, r_e is the pore radius (4.5×10^{-9} m), ε is the catalyst void ratio (0.4, also calculated from the adsorption isotherm), τ is the tortuosity factor, and M_A is the molecular mass of

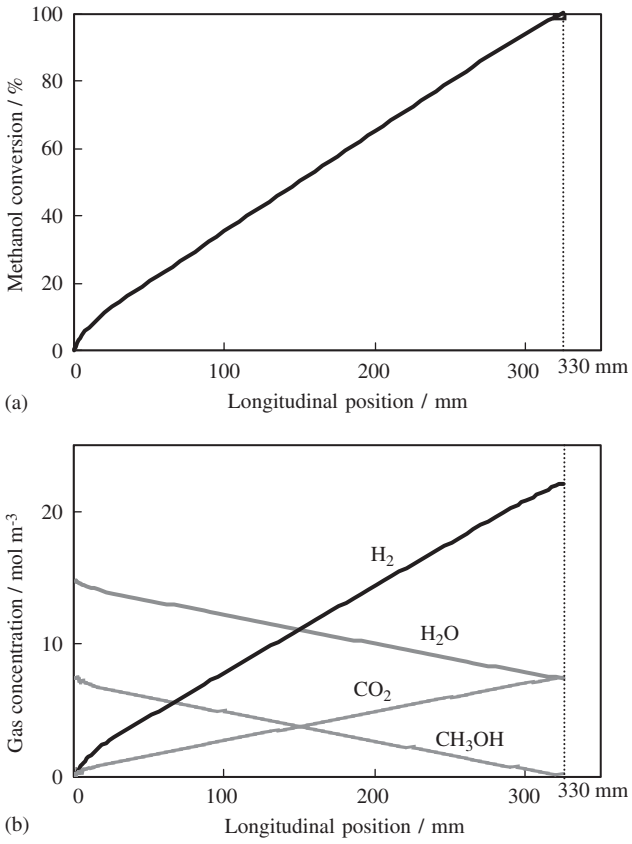

Fig. 4. Simulated (a) methanol conversion and (b) gas concentrations of reactants and products in direction of flow.

reactant A. The diffusion time of reactant A is expressed as Eq. (7).

$$t_{\mathrm{cat}A} = \frac{\delta^2}{D_{eA}}. \tag{7}$$

Fig. 5 shows the dependence of the calculated diffusion time for each reactant on the thickness of the catalyst layer under the assumption of $\tau = 4$, which is a reasonable value for normal porous catalysts. For comparison, Fig. 5 also includes the results for a residence time of 0.13 s at the typical flow rate of 1.0 ml h^{-1} (S/C = 2.0 mol mol^{-1}). At the designed thickness of the catalyst layer (15 μm), the residence time, corresponding to the reaction time, would be hundreds of times longer than the diffusion time. Furthermore, as the diffusion rate of gases in the cross-sectional direction of the microchannel can be expected to be sufficiently large compared to the rate of reaction (Yamamoto et al., 2002), diffusion limitations are considered to be negligible.

Based on the design derived above, the microchannel was arranged in a serpentine shape to minimize the size of the microreactor, which had final dimensions of $25 \times 17 \times 1.3$ mm^3.

The pressure drop and uniformity of temperature in the designed microreactor were estimated by computational fluid dynamics (CFD) simulations (Cradle, STREAM) (Yamamoto et al., 2002). Fig. 6 shows the simulated

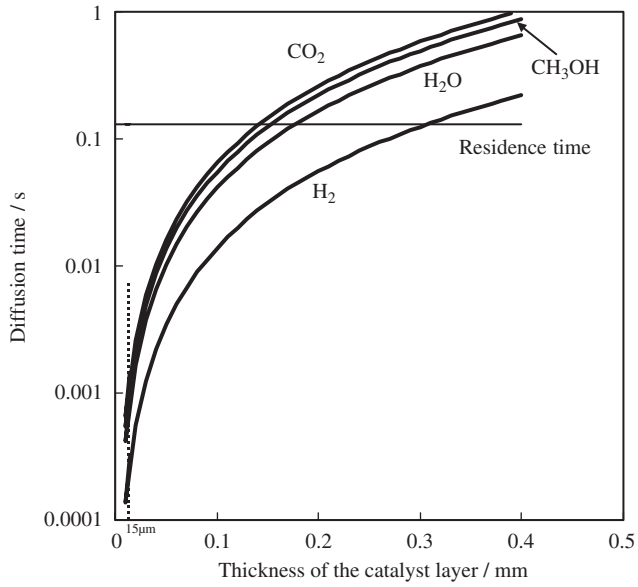

Fig. 5. Dependence of simulated diffusion time of each reactant in catalyst layer on thickness of catalyst layer.

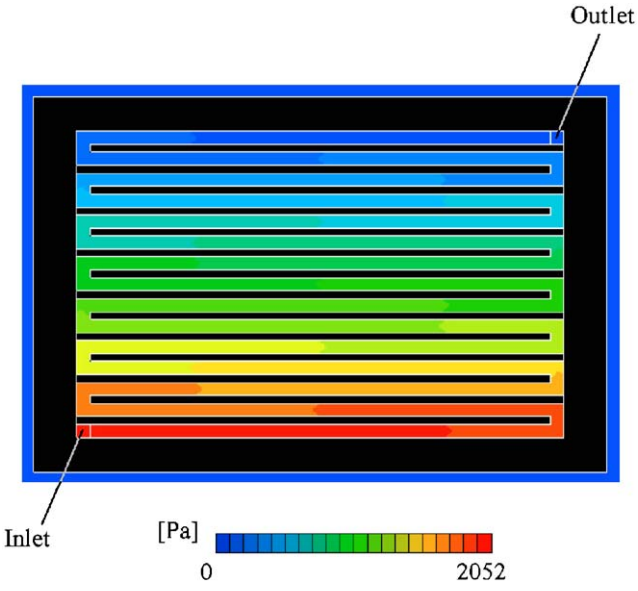

Fig. 6. Simulated pressure distribution in microchannel.

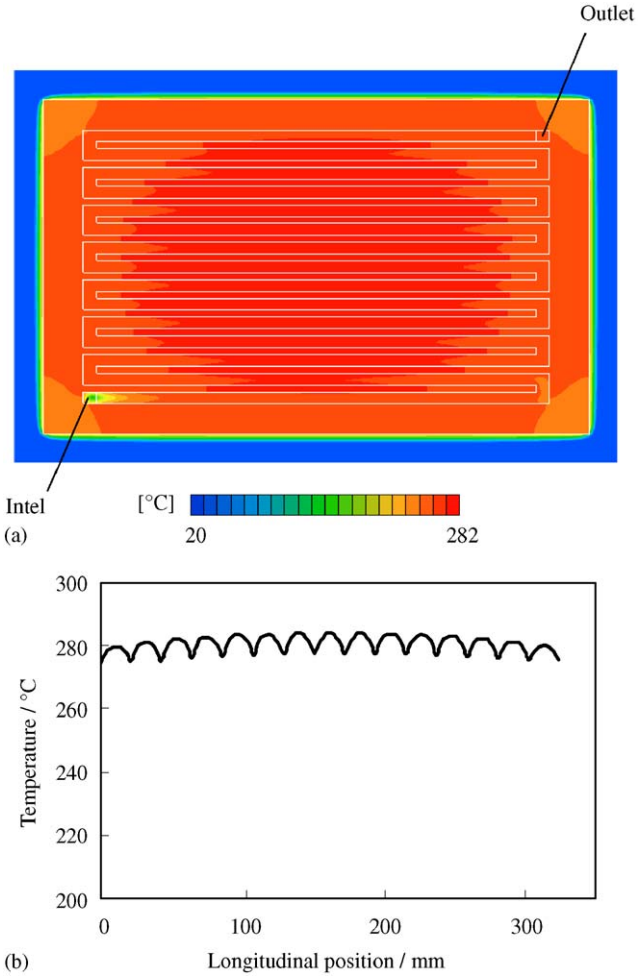

Fig. 7. Simulated temperature distribution in (a) planar direction on microchannel side and (b) direction of flow.

pressure distribution in the microchannel expressed as a pressure drop with respect to the pressure at the outlet. The simulation predict a low pressure drop ($\Delta P = 2052$ Pa) with laminar flow of $Re = 23$. Fig. 7 shows the temperature distributions in the planar direction on the microchannel side (Fig. 7(a)) and in the flow direction of the microchannel (Fig. 7(b)) predicted by a simulation of heat transfer to ambient air by natural convection and radiation (in addition to the heat consumed for chemical reaction). In the CFD simulation, the temperature distribution in the microreactor was calculated by

$$\frac{\partial u_i}{\partial x_i} = 0, \tag{8}$$

$$\frac{\partial \rho u_i}{\partial t} + \frac{\partial u_j \rho u_i}{\partial x_i} = -\frac{\partial P}{\partial x_i} + \frac{\partial}{\partial x_j}\mu\frac{\partial u_i}{\partial x_j} - \rho g_i \beta (T - T^0), \tag{9}$$

$$\frac{\partial \rho c_{\mathrm{pm}} T}{\partial t} + \frac{\partial u_j \rho c_{\mathrm{pm}} T}{\partial x_j} = \frac{\partial}{\partial x_j} K \frac{\partial T}{\partial x_j} + Q \tag{10}$$

for mass, momentum, and heat balance, respectively. These equations are commonly applied for incompressible fluid analysis. For CFD calculations, the microreactor was assumed to be placed in free space in the ambient atmosphere, and heat transfer to ambient air by natural convection and radiation was considered out to 50 mm from the surface of the microreactor. A large heat transfer coefficient (10^{10} J s^{-1} m^{-2} K^{-1}) was assigned at a hypothetical wall between the analyzed area and an external area as the boundary condition. Although a slight drop in temperature appears in a

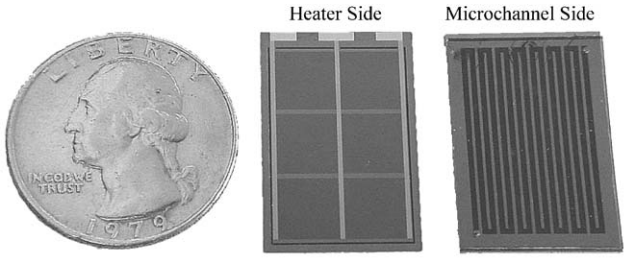

Fig. 8. Photographs of fabricated microreactor.

confined region near the inlet, the uniformity of temperature is excellent, within 10 °C over the majority of the reactor. The large diffusion rate of gases in the cross-sectional direction of the microchannel leads to minimize concentration distributions of gases to 1% or less (Yamamoto et al., 2002), which means the Dufour effect is negligible. These features suggested that the designed microchannel and microreactor should make the best use of the intrinsic performance of this catalyst for methanol reforming.

Fig. 8 shows the microreactor fabricated based on this design using the process flow shown in Fig. 2. The size of the microreactor is suitable for use as a power source for portable electronic devices.

3.2. Deposition of catalyst in microchannel

Fig. 9 shows SEM images of the microchannel wall, the Al_2O_3 boehmite layer, and the catalyst deposited in the microchannel. A microscale roughness due to sandblasting can be observed in Fig. 9(a), which may have provided an anchoring effect for the strong adhesion between the microchannel wall and the Al_2O_3 boehmite layer. Sandblasting is also a relatively quick process and can be performed several times faster than chemical etching using KOH (Kusakabe et al., 2001; Cui et al., 2000) or deep reactive ion etching (RIE) (Toda et al., 1998). This will facilitate mass production should the microreactor be applied widely as a power source for portable electronic devices. The Al_2O_3 boehmite layer (Fig. 9(b)), which was formed between the catalyst layer and the microchannel wall, is considered to provide this improved adhesive strength through affinity with the Al_2O_3 present in the catalyst as a support. Therefore, the catalyst layer was deposited in the microchannel wall with strong adhesion, with no defects such as peeling, as shown in Fig. 9(c).

Fig. 10 shows the results of SEM-EDX analyses of the microchannel. Analyses using Si–Kα and Cu–Lα beams reveal that the catalyst was selectively deposited only on the microchannel walls. Contamination of the Si surface adjacent to the microchannel with catalyst powder could introduce gaps between the Si and glass substrates during the junction process, resulting in incomplete contact and leading to gas leaks or bypassing of parts of the microchannel. Selective deposition of the catalyst layer in the microchannel is therefore

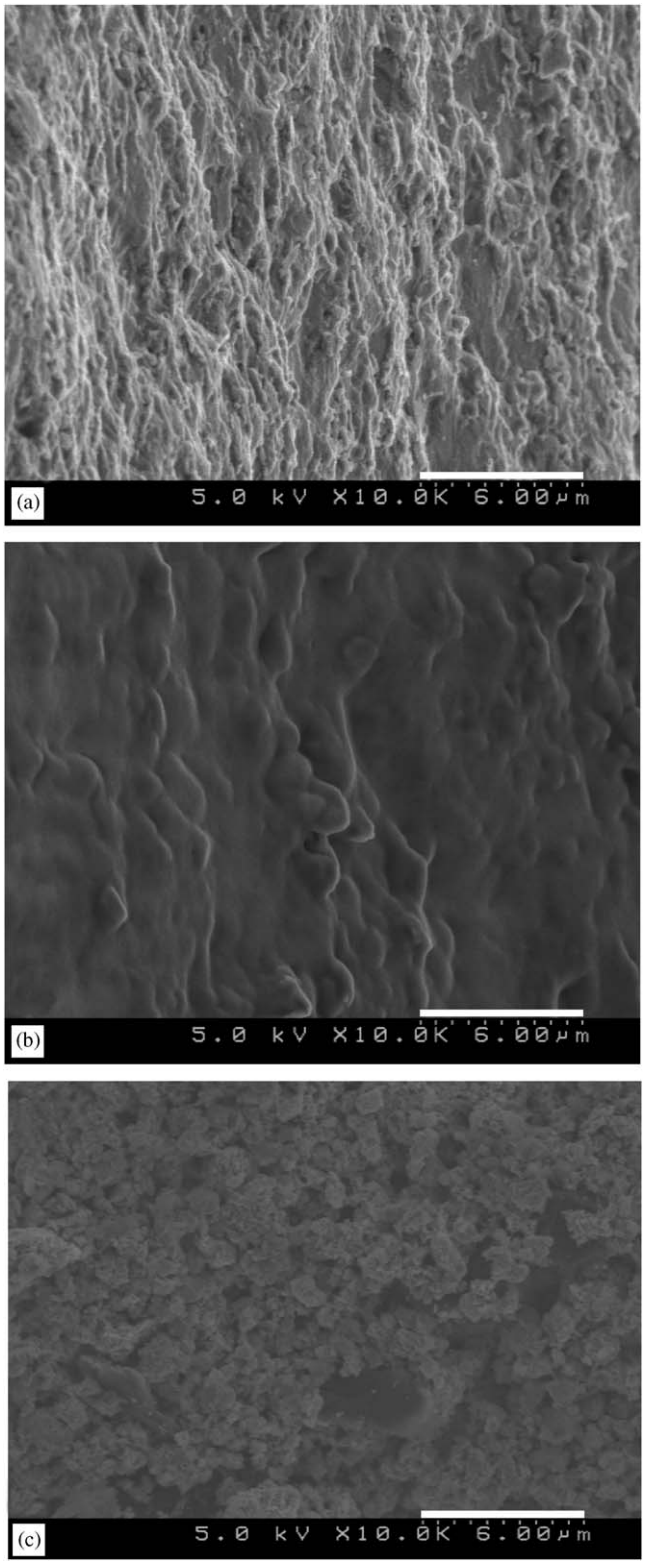

Fig. 9. SEM images of (a) microchannel wall, (b) Al_2O_3 layer in microchannel, and (c) catalyst layer.

very important for the fabrication of a quality microreactor. The catalyst deposition was also found to be uniform, with no exposed wall areas remaining after deposition (Fig. 10).

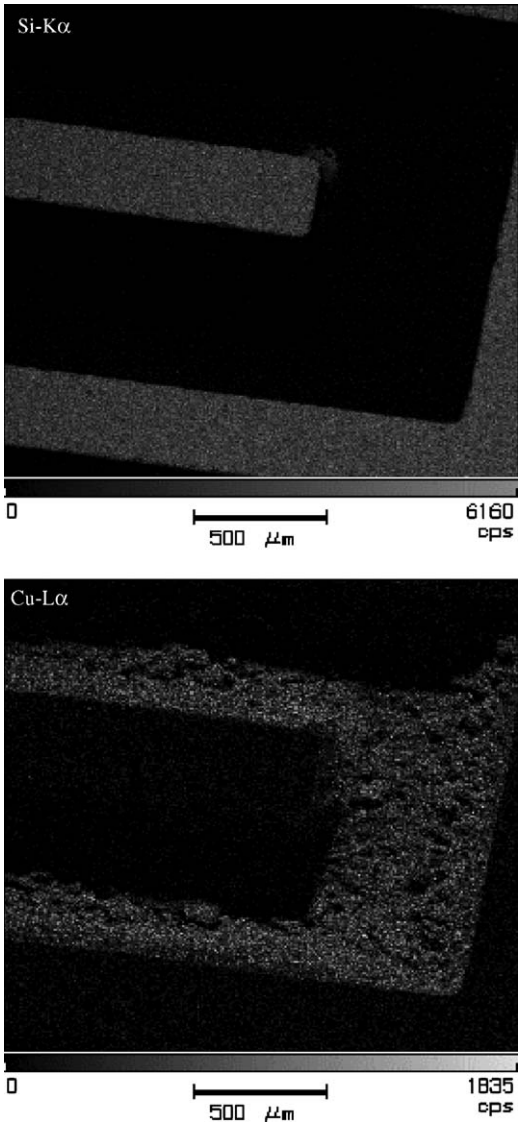

Fig. 10. SEM-EDX analyses of microchannel.

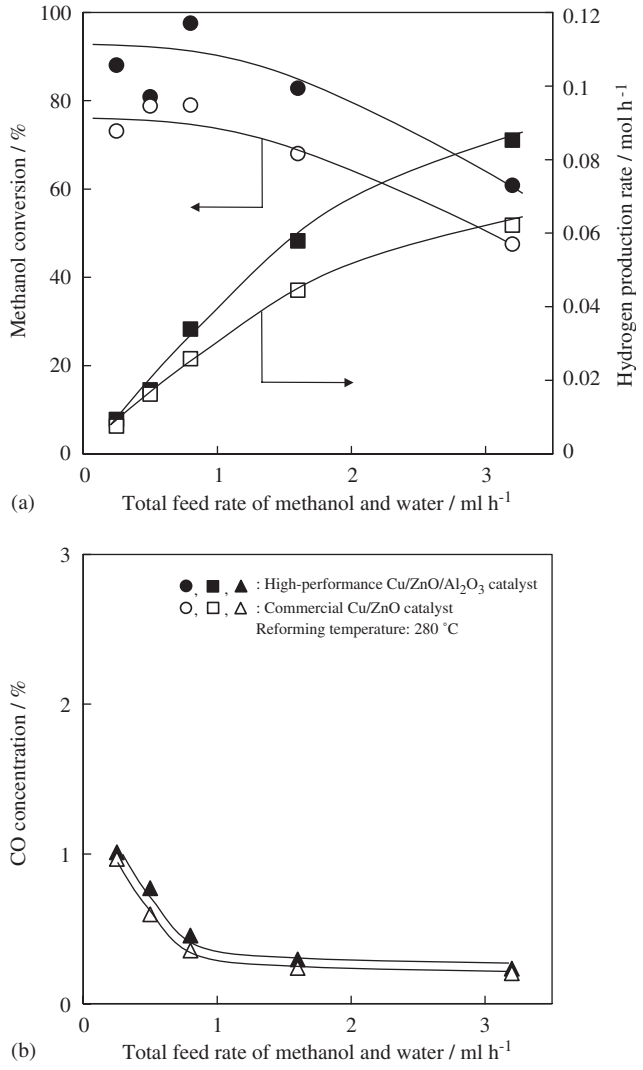

Fig. 11. Measured catalytic performances of microreactor in (a) methanol conversion and hydrogen production rate and (b) CO concentration.

3.3. Reforming characteristics of microreactor

Fig. 11(a) shows the methanol conversion and hydrogen production rates using this microreactor with the high-performance $Cu/ZnO/Al_2O_3$ catalyst in comparison to the results using the same reactor with a commercial catalyst measured at a microreactor temperature of 280 °C. Methanol conversion decreased with increasing feed rate of the reactant, whereas the hydrogen production rate increased. As found previously for a conventional fixed-bed flow reactor (Kawamura et al., 2005), the high-performance $Cu/ZnO/Al_2O_3$ catalyst exhibits superior catalytic activity to the commercial catalyst. However, although the simulations predicted that methanol should be converted completely to hydrogen and carbon dioxide at a flow rate of 1.0 ml h^{-1} over the high-performance $Cu/ZnO/Al_2O_3$ catalyst, the observed methanol conversion (Fig. 11(a)) did not reach 100%. As the distribution of gases exhibits only a slight lateral variation across the channel (Yamamoto et al., 2002), this lower rate of methanol conversion is considered not to be due to differences in residence time between gas in the center of the microchannel and that closer to the microchannel wall under laminar flow. Furthermore, slight differences in catalyst thickness (e.g., 14 μm based on the catalyst weight of 10 mg versus the assumed thickness of 15 μm simulations) have little effect on the predicted conversion at the outlet. In Jiang et al. (1993), from which the reaction orders in rate Eq. (2) are obtained, the reaction order in methanol was determined experimentally at methanol pressures exceeding 5 kPa to be 0.26. The methanol pressures of less than 3 kPa at 90% methanol conversion in the present study are beyond the range considered in that report. Under such low methanol partial pressure, the reaction order may be increased by a reduction in methanol coverage over the catalyst, which would make 100% conversion difficult to

achieve. Since the persistence of unreformed methanol can cause instability in subsequent CO removal process, it is preferable that methanol conversion be as close as possible to 100%. Further detailed kinetic analyses and optimization of the present microreactor design will therefore be necessary in order to achieve 100% methanol conversion.

Fig. 11(b) shows the observed CO concentrations in the reformed gases without liquid components. The CO concentrations of less than 1% detected under all experimental conditions are sufficiently low for a subsequent preferential oxidation of CO (PROX) process in a miniaturized PEMFC system, which has already been prototyped primitively in our correlative work (Ogura et al., 2002). The high-performance $Cu/ZnO/Al_2O_3$ catalyst produced slightly greater levels of carbon monoxide than the commercial catalyst. Generally, a Cu/ZnO catalyst for methanol steam reforming also performs for water gas shift reaction, in other words, reverse water gas shift reaction should proceed. Therefore, increase of CO concentration over a more active Cu/ZnO catalyst is inevitable.

The microreactor requires several watts of electrical power for heating to the operating temperature of 280 °C without thermal insulation, exceeding the predicted power generated by the microreactor system. Although the thermal efficiency of this microreactor system cannot be discussed based on the present experimental results, it is anticipated that housing in a suitable vacuum package will achieve methanol reforming with sufficiently low heat loss (Yamamoto et al., 2002; Terazaki et al., 2003). The construction of a vacuum package is thus considered essential to improving the thermal efficiency of the proposed system. Combination with catalytic combustion as a heat source by consumption of methanol or recycled hydrogen from the anode side of a PEMFC may allow further improvements in thermal efficiency to be realized.

Long-term and dynamic operating tests will also be required to confirm the durability and reliability of the proposed microreactor for practical use. Nevertheless, the present results demonstrate that a microreactor based on the $Cu/ZnO/Al_2O_3$ catalyst is capable of hydrogen production rates exceeding $0.05\,mol\,h^{-1}$ at a reactant feed rate of $1.6\,ml\,h^{-1}$. Based on the lower hydrogen heating value of $241 \times 10^3\,J\,mol^{-1}$, this hydrogen production rate corresponds to $3.3\,W_{th}$ of hydrogen power, in which electrical power greater than 1 W is expected assumed under 45% of fuel cell efficiency and 70% of hydrogen utilization in a PEMFC, making it potentially applicable as a power source for cellular phones.

4. Conclusions

In this study, a miniaturized methanol reformer having a $Cu/ZnO/Al_2O_3$ catalyst-based microreactor was developed as a hydrogen production unit for a small PEMFC. The microreactor consists of a catalyst-coated microchannel in a serpentine arrangement, with length of 333 mm and cross-sectional dimensions of $0.6 \times 0.4\,mm^2$. The length of the microchannel was determined by mass and heat balance equations based on a one-dimensional model. The designed microreactor should bring out the intrinsic performance of the $Cu/ZnO/Al_2O_3$ catalyst developed in our previous study for methanol steam reforming. The microreactor was fabricated from Si and glass substrates using a number of microfabrication techniques. Sandblasting was found to be suitable for microchannel formation, allowing the microchannels to be processed quickly and leaving a desirable surface (microscale roughness) for subsequent catalyst deposition. Catalyst adhesion is also promoted by the natural formation of an Al_2O_3 boehmite layer at the catalyst/substrate interface. Selective deposition of the catalyst in the microchannel was achieved by employing a photolithography technique, ensuring that complete contact is realized between the Si and glass substrates forming the reactor in the anodic bonding process. The overall size of the microreactor ($25 \times 17 \times 1.3\,mm^3$) makes this device suitable for application as a power source for portable electronic devices. Methanol reforming using this reactor was also demonstrated to reach the levels necessary to power 1 W-class small PEMFC systems, which is adequate, for example, to power a cellular phone. It remains necessary to refine this design to improve thermal efficiency and achieve 100% methanol conversion, which is necessary for practical application. Durability tests are also required in order to confirm the feasibility of this microreactor concept.

Notation

Symbols and constant

c_{pm}	fluid specific heat, $J\,kg^{-1}\,K^{-1}$
C_A	concentration of reactant A, $mol\,m^{-3}$
C_{A0}	concentration of reactant A at the inlet of the reactor, $mol\,m^{-3}$
D_{eA}	effective diffusion coefficient of reactant A, $m^2\,s^{-1}$
E_a	activation energy, $J\,mol^{-1}$
g_i	acceleration in x_i direction, $m\,s^{-2}$
h	cross-sectional depth of the microchannel, m
ΔH^0_{298}	standard heat of reaction, $J\,mol^{-1}$
ΔH_r	heat of reaction, $J\,mol^{-1}$
k_0	frequency factor, $mol\,kg^{-1}\,s^{-1}\,Pa^{-0.09^a}$
K	heat conductivity, $J\,m^{-1}\,s^{-1}\,K^{-1}$
M_A	molecular mass of reactant A, $kg\,mol^{-1}$
P	fluid pressure, Pa
ΔP	pressure drop, Pa
P_A	partial pressure of reactant A, Pa
q	heatflux, $J\,m^{-2}\,s^{-1}$
Q	heat value, $J\,m^{-3}\,s^{-1}$
r	rate of reaction, $mol\,s^{-1}\,m^{-3}$
r_A	rate of reaction of reactant A, $mol\,s^{-1}\,m^{-3}$
r_e	pore radius, m

r_{SR}	rate of methanol steam reforming reaction, mol s^{-1} m^{-3}
R	gas constant $= 8.314$ J mol^{-1} K^{-1}
t	time, s
$t_{\mathrm{cat}A}$	diffusion time in the catalyst layer of reactant A, s
T	temperature, K
T_0	temperature at the inlet of the reactor, K
T^0	standard temperature, K
u	flow rate of gases, m s^{-1}
u_0	flow rate of gases at the inlet of the reactor, m s^{-1}
u_i	flow rate in x_i direction, m s^{-1}
w	cross-sectional width of the microchannel, m
x_A	conversion of reactant A, dimensionless
x_i	position in i axis, m
z	longitudinal position from the inlet of the reactor, m

Greek letters

β	coefficient of cubical expansion, K^{-1}
δ	thickness of the catalyst layer, m
ε	catalyst void ratio, dimensionless
η	effectiveness factor of catalyst, dimensionless
μ	coefficient of viscosity, Pa s
ρ	fluid density, kg m^{-3}
ρ_{cat}	bulk density of the catalyst layer, kg m^{-3}
τ	tortuosity factor, dimensionless

Dimensionless group

Re	Reynolds number

[a] In the case of applying rate Eq. (2).

Acknowledgements

The authors gratefully acknowledge the assistance of Prof. Jiro Koga and Associate Prof. Shunji Honma of Saitama University for helpful advice on CFD simulations.

References

Cui, T., Fang, J., Zheng, A., Jones, F., Reppond, A., 2000. Fabrication of microreactors for dehydrogenation of cyclohexane to benzene. Sensors and Actuators B: Chemical 71, 228–231.

Dyer, C.K., 2002. Fuel cells for portable applications. Journal of Power Sources 106, 31–34.

Dyer, C.K., 2004. Fuel cells and portable electronics. 2004 Symposium on VLSI Circuits Digest of Technical Papers, pp. 124–127.

Ehrfeld, W., Hessel, V., Löwe, H., 2000. Microreactors. Wiley-VCH, Weinheim, Germany.

Holladay, J.D., Jones, E.O., Phelps, M., Hu, J., 2002. Microfuel processor for use in a miniature power supply. Journal of Power Sources 108, 21–27.

Hu, J., Wang, Y., VanderWiel, D., Chin, C., Palo, D., Rozmiarek, R., Dagle, R., Cao, J., Holladay, J., Baker, E., 2003. Fuel processing for portable power applications. Chemical Engineering Journal 93, 55–60.

Igarashi, A., 2002. Microreactor for heterogeneous catalysis. Kagaku Kogaku 66, 67–70 (in Japanese).

Jiang, C.J., Trimm, D.L., Wainwright, M.S., Cant, N.W., 1993. Kinetic study of steam reforming of methanol over copper-based catalysts. Applied Catalysis A: General 93, 245–255.

Kawamura, Y., Yamamoto, K., Ogura, N., Katsumata, T., Igarashi, A., 2005. Preparation of Cu/ZnO/Al_2O_3 catalyst for a micro methanol reformer. Journal of Power Sources, in press.

Kusakabe, K., Morooka, S., 2002. Chemical engineering for micro chemical plants. Kagaku Kogaku 66, 54–57 (in Japanese).

Kusakabe, K., Miyagawa, D., Gu, Y., Maeda, H., Morooka, S., 2001. Development of self-heating microreactor for catalytic reactions. Journal of Chemical Engineering of Japan 34, 441–443.

Lee, J.K., Ko, J.B., Kim, D.H., 2004. Methanol steam reforming over Cu/ZnO/Al_2O_3 catalyst: kinetics and effectiveness factor. Applied Catalysis A: General 278, 25–35.

Ogura, N., Kawamura, Y., Igarashi, A., 2002. Small PEMFC system with microreactor. In: Abstracts of the 2002 Fuel Cell Seminar, Palm Springs, CA, pp. 243–246.

Park, G.G., Seo, D.J., Park, S.H., Yoon, Y.G., Kim, C.S., Yoon, W.L., 2004. Development of microchannel methanol steam reformer. Chemical Engineering Journal 101, 87–92.

Pavio, J., 2003. Performance and design of a reformed hydrogen fuel cell system. In: Abstracts of the 2003 Fuel Cell Seminar, Miami Beach, FL, pp. 973–976.

Purnama, H., Ressler, T., Jentoft, R.E., Soerijanto, H., Schlögl, R., Schomäcker, R., 2004. CO formation/selectivity for steam reforming of methanol with a commercial CuO/ZnO/Al_2O_3 catalyst. Applied Catalysis A: General 259, 83–94.

Reuse, P., Renken, A., Haas-Santo, K., Görke, O., Schubert, K., 2004. Hydrogen production for fuel cell application in an autothermal microchannel reactor. Chemical Engineering Journal 101, 133–141.

Samms, S.R., Savinell, R.F., 2002. Kinetics of methanol-steam reformation in an internal reforming fuel cell. Journal of Power Sources 112, 13–29.

Takahashi, K., Takezawa, N., Kobayashi, H., 1982. The mechanism of steam reforming of methanol over a copper-silica catalyst. Applied Catalysis 2, 363–366.

Tanaka, Y., Takeyama, K., Nakamura, O., 2001. Development of TaSiON resister heater for use in thermal inkjet printheads. In: Extended Abstracts of the 62nd Autumn Meeting of the Japan Society of Applied Physics, Toyota, Japan, p. 142 (in Japanese).

Tanaka, S., Chang, K.S., Min, K.B., Satoh, D., Yoshida, K., Esashi, M., 2004. MEMS-based components of a miniature fuel cell/fuel reformer system. Chemical Engineering Journal 101, 143–149.

Tanaka, Y., Takeyama, K., Terazaki, T., Nakamura, O., 2005. Development of thin-film Ta–Si–O–N resistor heater. IEE Japan Transactions on Sensors and Micromachines 125, 355–363 (in Japanese).

Terazaki, T., Takeyama, K., Nakamura, O., Yamamoto, T., 2003. The improvement of thermal efficiency of micro methanol reformer for fuel cell. In: Preprints of the 68th Annual Meetings of the Society of Chemical Engineers, Japan, Tokyo, Japan, C114 (in Japanese).

Toda, R., Minami, K., Esashi, M., 1998. Thin-beam bulk micromachining based on RIE and xenon difluoride silicon etching. Sensors and Actuators A: Physical 66, 268–272.

Yamamoto, T., Honma, S., Koga, J., 2002. Reaction channel and thermal insulation design of micro methanol reformer for small PEMFC. In: Preprints of the 35th Autumn Annual Meetings of the Society of Chemical Engineers, Japan, Kobe, Japan, G206 (in Japanese).